Heliyon 7 (2021) e08368

Contents lists available at ScienceDirect

Heliyon

journal homepage: www.cell.com/heliyon

Research article

Nose to brain delivery of Efavirenz nanosuspension for effective neuro AIDS therapy: *in-vitro*, *in-vivo* and pharmacokinetic assessment

Smita Kakad *, Sanjay Kshirsagar

Department of Pharmaceutics, MET's Institute of Pharmacy, Nashik, Affiliated to Savitribai Phule Pune University, Pune, 422003, India

GRAPHICAL ABSTRACT

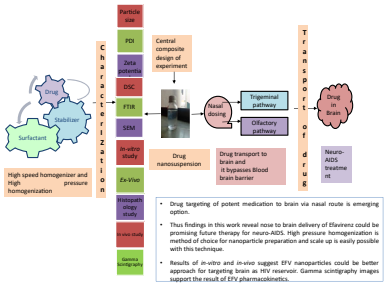

ARTICLE INFO

Keywords:
Blood brain barrier
Brain targeting
Efavirenz
Intranasal
Nanosuspension
Neuro-AIDS

ABSTRACT

Efavirenz is inhibitor of non-nucleoside reverse transcriptase enzyme; BCS class II drug. The objective of the present research was to prepare and evaluate nanosuspension of Efavirenz for the treatment of neuro-AIDS. Efavirenz is the substrate for drug resistant proteins at BBB prone to efflux and could not reach brain with effective levels. Current need of the therapy is to develop drug delivery systems targeting viral reservoirs at effective concentration in the brain. With this need we developed Efavirenz nanosuspension for nose to brain drug transport to bypass blood brain barrier. Nanosuspension prepared with high-pressure homogenization had a mean particle size of 223 nm, PDI of 0.2 and -21.2 mV zeta potential. Histopathology study on goat nasal mucosa showed no adverse effects of formulation on nasal tissues. Gamma scintigraphy study and *in-vivo* study on Wistar rat model reveals drug transport to the CNS after nasal administration. Pharmacokinetic parameters and drug targeting potential of 99.46 % suggest direct nose to brain transport of Efavirenz nanoparticle. Results reveal that nose to brain delivery of Efavirenz is the best possible alternative for neuro –AIDS treatment.

1. Introduction

UNAIDS (The Joint United Nations Programme on HIV and AIDS) report says that "Prevention and end of AIDS as a common health threat can be interpreted quantitatively as a 90% reduction in newly developed HIV infections and deaths caused by AIDS (Acquired Immunodeficiency Syndrome) elated illness by year 2030 compared to 2010 baselines." 25.4 million People were accessing antiretroviral therapy and 38 million people worldwide living with HIV indicate its huge prevalance [1, 2].

Invasion of human immunodeficiency virus (HIV) to central nervous system (CNS) is associated with neurologic condition called neuro-AIDS. Neuro-AIDS prevails among AIDS patients [3].

HIV gains entry into brain via blood-derived macrophages or trans-migration across blood brain barrier [4]. After entering into brain HIV

* Corresponding author.
E-mail address: smitadarade87@gmail.com (S. Kakad).

https://doi.org/10.1016/j.heliyon.2021.e08368
Received 30 April 2021; Received in revised form 23 August 2021; Accepted 8 November 2021

follows both pathophysiologic infectious pathway and degenerative pathway [5]. HIV associated neurocognitive disorders (HAND) are of three different categories as (a) Asymptomatic neurocognitive impairment, (b) Mild neurocognitive disorder and (c) HIV-associated dementia [6].

Alessandro et al (2018); reported that ARVs (anti-retroviral) show difficulties in penetrating BBB due to active efflux transporters (AETs). To avoid efflux of ARV via efflux transporters drug can deliver bypassing blood brain barrier [7]. EFV could not cross BBB efficiently after IV administration as active efflux transporter protein hinders in the transport of EFV at BBB. EFV is a substrates for breast-cancer-resistance protein (BCRP) active efflux transporters at BBB. EFV is a ligand of both human receptors nuclear pregnane X (PXR) and human constitutive androstane (hCAR). Nuclear receptor activity of EFV restricts its ability to enter the brain by increasing P-gp expression at BBB [7].

Nose to brain drug delivery via trigeminal and olfactory pathway is a success for migraine therapy and vaccine delivery, which may prove a better alternative for ARV to reach the brain with an effective drug level. The design of promising drug delivery approaches for life-threatening HIV infection may save the brain from Neuro-AIDS and help to enhance the socio-economic life of HIV patients [8]. Intranasal nanoformulations enhances drug bioavailability to the CNS as this route protects the drug from chemical and biological degradation, it prevents P-gp efflux proteins associated extracellular transport of drug, nano size of drug facilitates transcellular transport via neuronal pathway [9]. Thus nose to brain delivery of the antiretroviral may prove effective solution for treating neuro-AIDS pathogenesis.

EFV is non-nucleoside reverse transcriptase inhibitor (NNRTI). It is a first line medication in the treatment of HIV infection. EFV is BCS class II drug with poor solubility in water about 4 μg/mL, lipophilicity in terms of log p is 5.4, and limited oral bioavailability of 40–50%, with high intra and inter-individual variability of 19–24% and 55–58%, respectively [10, 11]. EFV is low molecular weight (315.67 g/mol) drug. Lipophilic molecules with molecular weights less than 1 kDa are rapidly and efficiently absorbed transcellularly across the nasal membrane [12, 13]. HIV-patients on oral EFV therapies possibly have lesser drug concentration in the CNS contributes to persistence of HAND [14].

2. Materials and methods

EFV was generously suplied by Mylan Laboratories (Nashik, India) as a gift sample. Hydroxypropyl methylcellulose Premium LV (HPMC E3) generously gifted by Colorcon Asia Pvt., Ltd. (Goa, India). Poloxamer 407 (P407) was purchased from Signet Chemicals Corporation Pvt., Ltd. (Mumbai, India). Sodium lauryl sulphate (SLS) was purchased from Sisco Research Laboratories Pvt., Ltd. (Mumbai, India). All other chemicals and solvents were of analytical grade. The experimental procedures on animal were conducted after the approval of institutional animal ethics committee (IAEC) as per the guidelines of the CPCSEA for care of laboratory animals. Approval number is MET-IOP-IAEC/2019–20/02.

2.1. Preparation of nanosuspensions

Nanosuspensions were prepared by high speed (IKA T25, Ultra Turrex) 45 min at 15000 rpm) and high pressure homogenization technique (Gea Niro Soavi, 750 barr pressure with 20 cycles). To establish the process of nanosuspension trial batches were prepared. Combination of HPMC and poloxamer 407 (stearic stabilizer) and SLS (surfactant) were used for the preparation of nanosuspension. Response surface methodology (RSM) with central composite design (quadratic model) was used for the optimization of nanosuspension (Design-Expert® software, version 12, Stat-Ease, Inc., Minneapolis, MN, USA) with 2 independent factors as mention in Table 1. According to the design, 13 runs including factorial points (4), central points (5) and axial points (4) were analysed. Dependant variables were screened for all the batches, these are particle size, PDI and zeta potential. The polynomial fitting quality was employed

Table 1. Independent variable factors of design with coded value.

Factor	Name	Minimum (-α)	Maximum (+α)	Coded Low(-1)	Coded High(+1)
A	Poloxamer 407	31.72	88.28	-1 ↔ 40.00	+1 ↔ 80.00
B	SLS	1.89	23.11	-1 ↔ 5.00	+1 ↔ 20.00

to quantify the effect of independent formulation variable A and B on the response variables Y with applied constraints. Quadratic model generated following Eq. (1):

$$Y = A + B + AB + A^2 + B^2 + A^2B + AB^2 + AB^2 + A^3 + B^3 \quad (1)$$

Where Y is the measured response and A, B are the independent formulation variables.

2.2. Lyophilization of nanosuspension

The optimized batch of formulation was processed for lyophilization, to further increase the stability of product. Mannitol (1%) was used as a cryoprotectant. Filled 20mL of nanosuspension in flint coloured vials having rubber stoppers and frozen in deep freezer at −75 °C for 24h. These frozen mass was freeze-dried in lyophilizer (Virtis Benchtop, Bombay, India) for 48 h to produce free flowing dry powder [15, 16].

2.3. Characterization of EFV nanosuspension

2.3.1. Determination of particle size, size distribution and zeta potential

Nanosuspensions were characterized for zeta potential, mean particle size, and polydispersity index (PDI) by dynamic light scattering (DLS) method using the Malvern Zetasizer (Malvern Instruments Ltd. version 6.20, UK). Samples were suitably diluted with the double distilled water before analysis.

2.3.2. Morphology of nanosuspension

The scanning electron microscope (Supra 55- Carl Zeiss, Germany) with focused electron beam was utilized for the visualization of shape and morphology of the prepared nanosuspension [17].

2.3.3. DSC study

Thermal analysis of pure EFV and freeze-dried product using DSC (DSC 60, Shimadzu, Japan). The sample scanning rate of 20 °C/min over a temperature of 35–300 °C.

2.3.4. X-ray powder diffraction characterization

Crystalline structure of API and potential changes in the freeze dried nanosuspension were analysed by X-ray powder diffractometer (XRD-7000, Shimadzu, Japan) [16, 18].

2.3.5. Determination of saturation solubility

To determine saturation solubility added an excess amount of EFV and freeze dried nanosuspension separately in distilled water, to obtain a saturated solution. Samples were agitated in orbital shaker (Remi Electrotechnik) for 48 h at 25 °C. After centrifugation and filtration through a 0.1 mm membrane filter (Millipore Corporation), the filtrate was diluted and analysed at 247nm with UV spectrophotometer [19].

2.3.6. Nasal mucociliary transport time

As per approved animal study protocol rats were anesthetized by intramuscular injection of Ketamine 50 mg/ml IP. Animals were divided in two group (Test and control). Instilled 20 μL of test formulation added with the solution of methylene blue to a rat nose (5 mm depth into the right nostril) using a micropipette (Labline, ECO). The appearance of the dye at the pharynx and nasopalatine region of the oral cavity was recorded as the appearance time by taking swab with moistened cotton-

tipped applicators. For control group instilled normal saline added with methylene blue dye (5 mg/mL) and the appearance time of the blue dye was recorded [20, 21].

2.3.7. Nasal histopathology study

Histopathological studies were performed on goat nasal mucosa to check safety of the formulation when administered intranasal. Goat nasal mucosa was collected from a local slaughter house and placed in phosphate buffer solution (pH 6.5). It was cleaned with phosphate buffer and cut into nine symmetrical pieces with uniform thickness. The first 3 pieces were treated with formulation and the next 3 pieces were treated with the positive control 70% isopropyl alcohol, while the last three pieces were treated with negative control (PBS 6.5). After 1 h of treatment, all samples were washed thoroughly with phosphate buffer solution and stored directly in 10% solution of formalin for 24 h. It was important to ensure that the volume of formalin used was ten times more than the volume of the fixed sample. After 24 h, the formalin solution was replaced with 70 % ethanol and the samples stored at 4 °C for dehydration. The dehydrated sections were then embedded in agar and paraffin block and cut to 5 μm thickness by using a microtome. Finally, the samples were stained with a combination of haematoxylin and eosin (H&E) dye and observed under optical microscope to detect any damage [22].

2.3.8. In-vitro drug release study

The nanosuspension equivalent to 10 mg EFV was placed in a cellulose dialysis bag, (MWCO 12,000 g/mol; Himedia Laboratories Pvt. Ltd.), this was then sealed at both ends and immersed into a dialysis reservoir containing 150 mL phosphate-buffered saline (PBS, pH 6.5) preconditioned and maintained at 34 ± 0.5 °C on a water bath. Withdrawn 1 mL sample at specified time intervals (5, 15, 30, 45 and 60 min) and added same amount of fresh PBS to monitor sink conditions. Cumulative drug release was determined [21].

2.3.9. In-vivo drug release study

All the procedures related to animal handling were followed as per the approved animal study protocol. Animals were acclimatized to animal house facility for 2 week with 12 h light/dark cycle and temperature of 22 ± 2 °C. Animals were divided into two groups. Group A (Positive control) was injected via tail vein (IV) and group B (Test) was administered intranasal (IN). Further, animals from each group were studied for six time points (1, 4, 6, 12, 24, and 72h) with three rats in each group. Mild anaesthesia was given with Ketamine 50 mg/mL prior to intranasal dosing.

20μL dose (equivalent to 4 mg/kg of drug) was instilled in each nostril using micropipette. At fixed time intervals, blood specimens were collected in EDTA-coated tubes by retro-orbital puncture under mild anaesthesia and immediately brain were excised from the sacrificed animal. The collected blood was centrifuged at 8000 rpm/10 min/4 °C, plasma was separated and preserved at −20 °C. Homogenized brain samples in phosphate buffer saline and acetonitrile in the ratio of 50:50; followed by the centrifugation at 12000 rpm/15 min/10 °C. The clear liquid separated and preserved at −20 °C [23, 24, 25, 26, 27, 28, 29]. Further, samples were analysed with previously developed and validated RP-HPLC method [30].

Pharmacokinetic parameters c_{max}, t_{max}, t_{half} and AUC were determined. Drug targeting index and % drug transport were determined to check brain targeting potential. Eqs. (2), (3), (4), and (5) were used for calculation.

$$\text{Drug targeting index} = \frac{(\text{AUC brain}/\text{AUC plasma})\ \text{in}}{(\text{AUC brain}/\text{AUC plasma})\text{iv}} \quad (2)$$

$$\frac{\text{Biv}}{\text{Piv}} = \frac{\text{Bx}}{\text{Pin}} \quad (3)$$

$$\text{Bx} = \left(\frac{\text{Biv}}{\text{Piv}}\right) \times P_{in} \quad (4)$$

$$\%\text{DTP} = \frac{(\text{Bin} - \text{Bx})}{\text{Bin}} \times 100 \quad (5)$$

AUC_0-t of EFV after intravenous and intranasal administration in the brain and the plasma are Biv, Piv, Bin, Pin respectively. Bx is the AUC fraction of EFV in brain obtained after intranasal dosing it might come up with systemic circulation via blood brain barrier [31].

2.3.10. Gamma scintigraphy study

In-vivo biodistribution of drug was studied by gamma scintigraphy. The experimental procedures were conducted after the approval of institutional animal ethics committee (IAEC) as per the guidelines of the CPCSEA for care of laboratory animals. Nine healthy male Wistar rats (180–250g, aged 2–3months) were selected for this study. Animals were grouped as mentioned in Table 2; rats from first group were administered with intravenous EFV solution, animals from second group were administered with nasal dosing of EFV solution and third group was administered with nasal formulation. Drug solution (prepared in 0.9% saline solution and 30% propylene glycol as a co-solvent) added with reducing agent stannous chloride 20 min prior to radio labelling with 99mTc (1mci) by direct labelling method. Similarly drug nanosuspension (equivalent to 25 mg/mL drug) was radiolabelled. Incubated both mixtures for 30 min [7, 31]. Forty microliter of radiolabelled 99mTC- drug solution (1mg drug) was intravenously administered by tail vein of Wistar rat using 1-mL Helminton syringe, while radiolabelled 99mTC- drug solution (40μL) and 99mTc- drug nanoparticles (40μL) were administered intranasal in both nostrils using micropipette adaptor. Animals were held at supine positon with 90° angle for the deposition of maximum dose at olfactory region. Rats were anesthetized using ketamine 50 mg/mL and placed on the imaging platform. Radio images were taken at predetermined time interval (1hr, 2hr and 6hr) using gamma camera (Tandem_Discovery_630) at HCG Manvata Cancer Centre, Nashik, India. In between gamma scanning intervals, the animals were freed and allowed for normal activities [7, 31]. All the procedures involved in Gamma scintigraphy studies, were performed at nuclear medicine section of HCG Manvata Cancer Centre, Nashik, India.

2.3.11. Stability study

EFV-LNS (Efavirenz lyophilized nanosuspension) were analysed under accelerated stability conditions as per ICH guidelines. Sample was kept at temperature of 40 °C ± 2°C/and humidity of 75% RH ± 5% RH. Physical stability was assessed by checking zeta potential and particle size. Chemical stability was confirmed by analysing drug content of EFV-LNS [32].

3. Results

Process variables number of homogenization cycles and pressure were kept constant after taking trial batches and effect of formulation variables were analysed. Trial batches suggest the combination of HPMC 3cps, poloxamer 407 and SLS for better stabilization to EFV nanosuspension measured in terms of zeta potential. Nanosuspension batches prepared were as mention in Table 3.

Table 2. Animals grouped for gamma scintigraphy study.

Group Code	Compound No.	Dose (mg/kg)	No. of animals	Route
I	Drug solution	4	3	Intravenous
II	Drug solution	4	3	Intranasal
III	Drug formulation	4	3	Intranasal

Table 3. Batches prepared by high pressure homogenization.

Batch	Drug mg	HPMC 3cps mg	Poloxamer 407 mg	SLS mg	Particle size (Z- Avg nm)	PDI	Zeta potential (mV)
1	100	100	60	12.5	223.3	0.262	-21.2
2	100	100	80	20	146	0.414	-12.3
3	100	100	40	5	248.3	0.596	-7.09
4	100	100	12.5	31.71	223.2	0.431	-9.25
5	100	100	60	12.5	223.3	0.262	-21.2
6	100	100	88.28	12.5	423.4	0.630	-0.835
7	100	100	60	12.5	223.3	0.262	-21.2
8	100	100	60	12.5	223.3	0.262	-21.2
9	100	100	60	23.10	191.4	0.554	-11.8
10	100	100	60	1.89	364.3	0.716	-10.6
11	100	100	40	20	119.5	0.59	-10.5
12	100	100	60	12.5	223.3	0.262	-21.2
13	100	100	80	5	149.2	0.615	-7.78

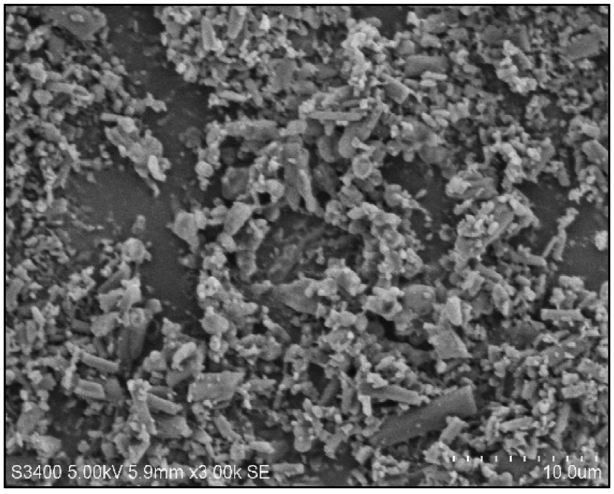

Figure 1. SEM of EFV-LNS

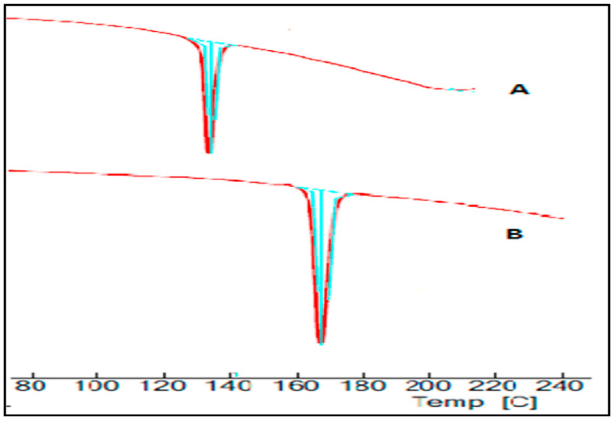

Figure 2. DSC thermogram of EFV (A) and EFV-LNS (B).

3.1. Influence of formulation variables on particle size, polydispersity index (PDI) and zeta potential

Polynomial Eqs. (6), (7), and (8) showing effect of variables on response.

$$\text{Particle size} = +223.30 + 26.32A - 47.06B + 31.40AB + 16.29A^2 - 6.43B^2 \quad (6)$$

$$\text{PDI} = +0.2620 + 0.0156A - 0.0545B - 0.0487AB + 0.127A^2 + 0.1793\ B^2 \quad (7)$$

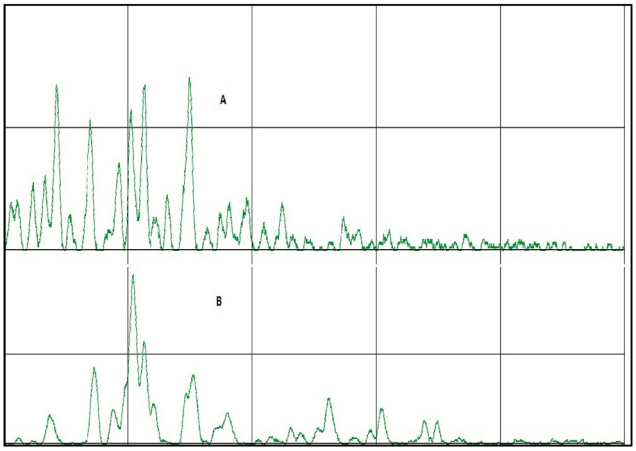

Figure 3. XRD spectra of EFV (A) and EFV-LNS (B).

$$\text{Zeta potential} = -21.20 + 1.18A - 1.20B - 0.2775AB + 7.75\ A^2 + 4.68\ B^2 \quad (8)$$

Poloxamer concentration (A) and SLS concentration (B) both formulation variables shown significant impact on zeta potential and particle size as compared to PDI. Refer Table 3 for the observation. PDI for nanoparticles was found in the range of 0.262–0.716. F1 formulation with particle size 223.3 nm, PDI of 0.262 and zeta potential -21.2 mV with desirability one was selected as the optimized batch. Optimized formulation F-1 with desirability one was found in good agreement with the predicted values generated by model with applied constraint.

3.2. Characterization of lyophilized EFV nanosuspension

3.2.1. Drug content, pH and saturation solubility

EFV content of the lyophilized product was found to be 96.56 ± 0.85. The apparent pH of the formulation was in the range of 6–6.5. Saturation solubility of lyophilized product was found to be 110.43 ± 0.8 μg/ml whereas the plain drug solubility was 6.97 ± 0.01 μg/ml in distilled water.

3.2.2. Morphology of nanosuspension

Scanning electron microscopy (SEM) image of optimized batch is revealed in Figure 1. It showed clusters of amorphous product after lyophilization rather than crystalline form of pure drug.

3.2.3. Differential scanning calorimery (DSC)

Figure 2 shows DSC thermogram of EFV lyophilized nanosuspension and EFV. Sharp melting endothermic peak of EFV was observed at 141.63

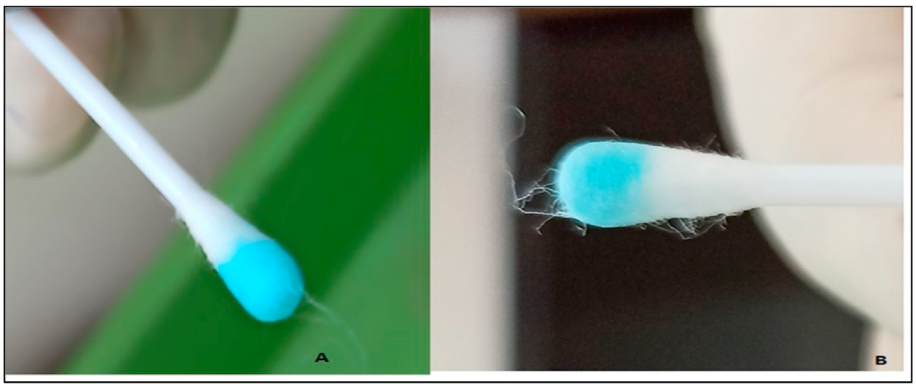

Figure 4. (A) Control solution swab collected after 2min and (B) formulation swab collected after 30 min.

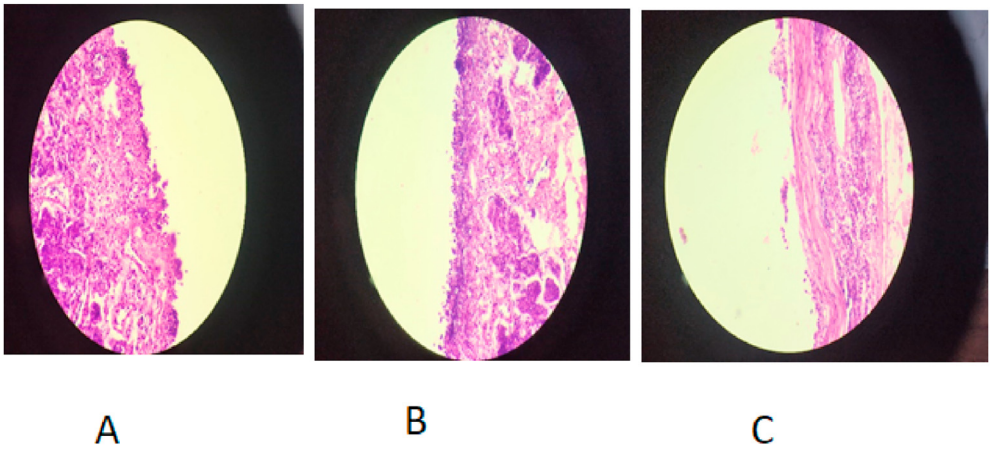

Figure 5. Histopathology study of EFV-LNS. (A: Formulation, B: Negative Control and C: Positive Control).

°C. Characteristic endothermic peak of EFV was absent in the DSC thermogram of EFV-LNS as drug was converted to amorphous form. EFV LNS thermogram showed endothermic peak at 171 °C corresponding to the melting point of mannitol used for lyophilization [34].

3.2.4. X-ray powder diffraction characterization (XRD)

Figure 3 shows XRD spectra of EFV and EFV-LNS. Characteristics multiple sharp peaks in the XRD spectrum of EFV at 2Θ = 14, 2Θ = 21 and 2Θ = 24 showed crystalline nature of EFV. XRD spectra of EFV LNS showed broad peaks at 2Θ = 17, 2Θ = 20 and 2Θ = 21. Absence of characteristics sharp peak of EFV indicates loss of crystalline nature of drug during formulation as it was converted to amorphous form [34].

3.2.5. Nasal mucociliary transport time

Nasal mucociliary transport time was observed between 27 to 32 min for the test formulation. It showed better residence of formulation in the nasal cavity [35]. Figure 4 showed images for swab after nasal administration of sample.

Table 4. Pharmacokinetic analysis.

Parameter	Plasma (IV)	Plasma (IN)	Brain (IV)	Brain (IN)
	Solution	NPS	Solution	NPS
C_{max}(μg/ml)	125.97 ± 2.61	6.65 ± 0.16	0.725 ± 0.002	4.49 ± 0.001
$T_{max\ (min)}$	15 ± 0.00	240 ± 0.00	360 ± 0.00	360 ± 0.00
$AUC_{0\text{-}72}$(μg/ml)*hr	856.33 ± 19.66	68.8 ± 1.26	8.427 ± 0.12	127.63 ± 0.23
$t_{half\ (hr)}$	18.4358 ± 0.12	13.977 ± 0.1058	14.1315 ± 3.1054	15.5931 ± 0.2622
$MRT_{(hr)}$	26.6802 ± 0.264	20.1621 ± 0.1537	19.6518 ± 5.001	22.4202 ± 0.4283

3.3. Nasal histopathology study

As shown in Figure 5C the positive control (70% isopropyl alcohol) shows changes in the epithelium cell i.e. they were detach from the membrane and also the regular sequence of the epithelium cells were distorted as compared to the negative control (Figure 5B). There was no significant destructive effect seen in the epithelial cell membrane after treated by EFV-LNS. So there was no damage to the mucosal cells seen in Figure 5C. Observations confirmed that the formulation found safe and non-irritant on intranasal administration [22].

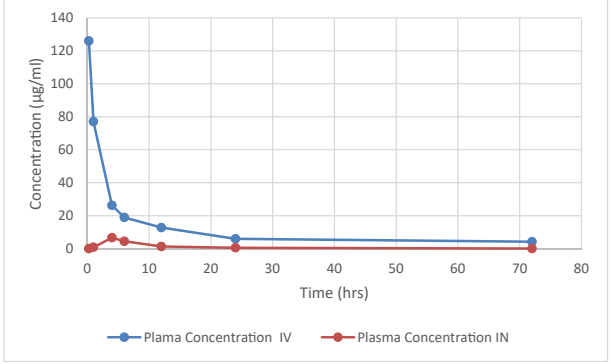

Figure 6. Plasma EFV concentration profile after IV and IN dose administration.

3.3.1. In-vitro drug release study

The *in-vitro* drug release study was performed using dialysis bag showed more than 81% cumulative drug released after 30 min. Mathematical models were applied to analyze the data for the drug release kinetics. Higuchi model was best fitted with the r^2value of 0.9546. Higuchi model reveals diffusion control drug release. The suspended nanoparticles showed better release profile with the polymer HPMC.

3.3.2. In-vivo drug release study

Pharmacokinetics of EFV after intravenous and intranasal administration were assessed by non-compartmental analysis and results are mentioned in Table 4. Figures 6 and 7 reveals comparison between plasma and brain EFV concentration.

C_{max} for brain after intranasal administration was significantly higher than obtained after IV dosing. $AUC_{0\text{-}72}$ of brain after intranasal administration was six fold higher than intravenous administration. Plasma $AUC_{0\text{-}72}$ of 68.8 ± 1.26 μg/mL*h showed partial drug transport to the systemic circulation absorbed via respiratory circulation. After IV administration $AUC_{0\text{-}72}$ of brain was small compared to plasma $AUC_{0\text{-}72}$ might be due to protein binding of EFV (>99.5%) and efflux by BCRP (breast cancer-resistant protein) present at brain endothelium [35]. The brain AUC fraction (Bx) contributed by systemic circulation after intranasal dosing was 0.68. Drug targeting index of 186.58 and drug targeting potential of 99.46 % suggest direct transport of EFV nanoparticle [31].

3.3.3. Gamma scintigraphy study

Gamma scintigraphy results reflect biodistribution of radiolabelled EFV. Figure 8 clearly depicts high radioactivity in the brain region after IN administration of nanoparticles as compared to IV drug solution. After IV dosing radioactivity was seen in abdomen at about 2 h of administration and later it diminishes up to 6 h.

3.3.4. Stability studies

Physical stability of nanosuspension was confirmed with insignificant changes observed in zeta potential and particle size. EFV-LNS found chemically stable as drug content of the formulation was observed unchanged during accelerated stability study. Table 5 gives results obtained after stability study.

4. Discussion

Optimum blend of stearic and electrostatic surfactant is required to produce the stable nanosuspension. HPMC and poloxamer 407 were good combination for stearic stability of nanosuspension also it has mucoadhesive properties required for good retention time [21, 35]. SLS was electrostatic stabilizer in the formulation [36]. Low PDI values of NPs indicate that the NPs with the narrow size range can be obtained with the size range of 119.5nm–423.4 nm are obtained in experiments performed.

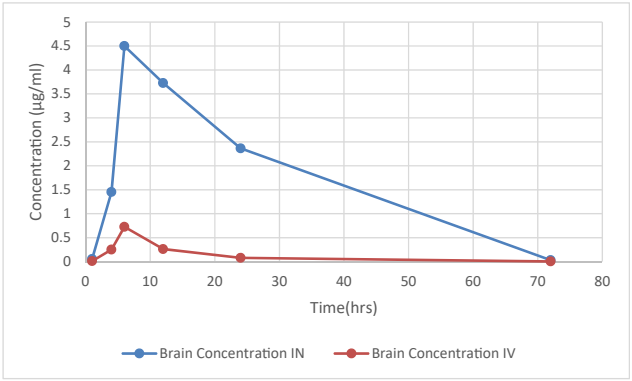

Figure 7. Brain EFV concentration profile after IV and IN dose administration.

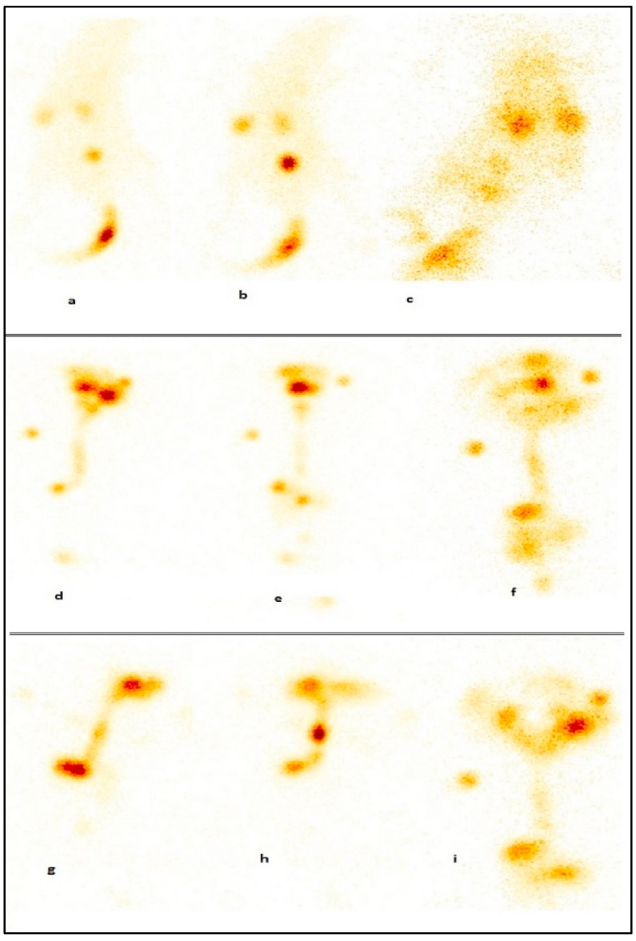

Figure 8. Gamma scintigraphy images of rat after intravenous administration of radiolabeled EFV solution (a = 1hr, b = 2hr, c = 6hr). Images of rat after intranasal administration of radiolabeled EFV nanosuspension (d = 1hr, e = 2hr, f = 6hr). Images of rat after intranasal administration of radiolabeled EFV solution (d = 1hr, e = 2hr, f = 6hr).

EFV is lipophilic and low molecular weight drug thus nanoparticle facilitates faster mucosal transport and transcellular transport via trigeminal pathway. Presence of both positive and negative charges at the surface of cell gives high binding affinity to NPs due to electrostatic interactions. Negatively charged nanoparticles bind at positively charged domains of cell membrane facilitates endocytosis and cell uptake. Nanoparticles could rapidly cross the mucosal barrier due to small size and charges developed on the surface [37]. Zeta potential values were dramatically affected with surfactant and stabilizer concentration as reported in Table 1. Zeta potential > ±20mV is required for stable nanosuspension [33]. Larger value for zeta potential (either negative or positive) imparts repulsion between suspended particles and prevents aggregate formation.

Lyophilized nanosuspension found with 15 fold increase in solubility as compared to pure EFV. This increase in the solubility was associated with conversion of drug to amorphous form and nanosizing of drug [19].

DSC, SEM and XRD study reveals that the lyophilized EFV nanoparticles are amorphous in nature [34]. Nasal mucocilliary clearance

Table 5. Stability study.

Sr. no.	Parameter	0 month	6 months
1	Drug content	90.55 ± 2.12	88.60 ± 2.02
2	Particle size nm	223.3	224.1
3	Zeta potential mV	-21.5	-19.1

study reveals that mucoadhesive nature and viscosity of the formulation achieved with polymer HPMC prolongs its retention in nasal cavity [35]. Drug transport may occur extracellularly from perineural spaces present around olfactory axons. Drug transport to CFS occurs via tight junctions at epithelium of olfactory nerves and connected in submucosa and subarachnoid space [38]. Drug transport is combination of olfactory and trigeminal pathway. Drug transported by passive diffusion from axons to olfactory bulb by endocytosis and pinocytosis.

Intranasal (IN) administration showed better CNS uptake of EFV NPS contributed by direct transport to CNS via trigeminal and olfactory region which bypasses BBB. Brain concentrations found higher than IC90-95 value of EFV [31, 39]. Drug targeting index and findings of *in-vivo* study suggest nose to brain delivery is promising strategy for neuro-AIDS treatment. Gamma scintigraphy supports the in vivo study and shown transport of drug to brain via nasal route.

5. Conclusion

For drug targeting of potent medication to brain nasal route is emerging option. Hurdles in nanosuspension development could be solved with selection of smart excipient. High pressure homogenization is method of choice for nanoparticle preparation and scale up is easily possible with this technique. Results of *in-vitro* and *in-vivo* suggest EFV nanoparticles could be better approach for targeting brain as HIV reservoir. Gamma scintigraphy images support the result of EFV pharmacokinetics. Thus findings in this work reveal nose to brain delivery of antiviral medication could be promising future therapy for neuro-AIDS.

Declarations

Author contribution statement

Smita Kakad: Conceived and designed the experiments; Performed the experiments; analyzed and interpreted the data; Contributed reagents, materials, analysis tools or data; Wrote the paper.

Sanjay Kshirsagar: Conceived and designed the experiments; Analyzed and interpreted the data; Contributed reagents, materials, analysis tools or data.

Funding statement

This research did not receive any specific grant from funding agencies in the public, commercial, or not-for-profit sectors.

Data availability statement

Data will be made available on request.

Declaration of interests statement

The authors declare no conflict of interest.

Additional information

No additional information is available for this paper.

Acknowledgements

Authors are thankful to Mylan Laboratories, (Sinnar), Nashik for providing API as a gift sample and Dr. Chaitanya Borde (Nuclear Scientist) at HCG Manavta Cancer Center, Nashik for providing radiolabeling and scintigraphy platform for conduction of animal study. Authors would like to thanks Mr. Rohan Pawar, RAP Analytical Nashik, for assistance during the conduction of bioanalytical study.

References

[1] Global HIV & AIDS Statistics-2018 fact sheet, Available at: https://www.unaids.org/en/resources/fact-sheet. (Accessed 25 March 2019).
[2] Global HIV & AIDS statistics-2020 fact sheet, available online at: https://www.unaids.org/en/resources/fact-sheet. (Accessed 27 December 2020).
[3] M. Nair, R.D. Jayant, A. Kaushik, et al., Getting into the brain: potential of nanotechnology in the management of neuro-AIDS, Adv. Drug Deliv. Rev. 103 (2016) 202–217.
[4] C.F. Pereira, H.S.L.M. Nottet, The blood-brain barrier in HIV-associated dementia, NeuroAids 3 (2000) 2.
[5] P. Shapshak, P. Kangueane, R.K. Fujimura, Editorial neuro-AIDS review, AIDS 25 (2011) 123–141.
[6] R. Vazeux, N. Brousse, A. Jarry, et al., AIDS subacute encephalitis: identification of HIV-infected cells, Am. J. Pathol. 126 (1987) 403–410.
[7] A. Dalpiaz, B. Pavan, Nose-to-Brain delivery of antiviral drugs: a way to overcome their active efflux, Pharmaceutics 10 (2) (2018) 39.
[8] S.P. Kakad, S.J. Kshirsagar, Neuro-AIDS: current status and challenges to antiretroviral drug therapy (ART) for its treatment, Curr. Drug Ther. 15 (2020) 1.
[9] A. Mistry, S. Stolnik, L. Illum, Nanoparticles for direct nose-to-brain delivery of drugs, Int. J. Pharm. 379 (2009) 146–157.
[10] C. Marzolini, A. Telent, L. Decostered, et al., Efavirenz plasma levels can predict treatment failure and central nervous system side effects in HIV-1-infected patients, AIDS 15 (2001) 1193–1194.
[11] D.A. Chiappetta, C. Hocht, J.A. Opezzo, et al., Intranasal administration of antiretroviral-loaded micelles for anatomical targeting to the brain in HIV, Nanomedicine 8 (2013) 223–237.
[12] C.A. Lipinski, F. Lombardo, B.W. Dominy, P.J. Feeney, Experimental and computational approaches to estimate solubility and permeability in drug discovery and development settings, Adv. Drug Deliv. Rev. 23 (1997) 3–25.
[13] Topical applications and the mucosa, in: C. Surber, P. Elsner, M.A. Farage (Eds.), Curr. Probl. Dermatol. 40 (2011) 20–35.
[14] M. Boyd, P. Reiss, The long-term consequences of antiretroviral therapy: a review, J. HIV Ther. 11 (2) (2006) 26–35.
[15] S. Taneja, S. Shilpi, K. Khatri, Formulation and optimization of efavirenz nanosuspensions using the precipitation-ultrasonication technique for solubility enhancement, Artificial Cells, Nanomed. Biotechnol. 44 (3) (2016) 978–984.
[16] P. Ige, R. Baria, S. Gattani, Fabrication of fenofibrate nanocrystals by probe sonication method for enhancement of dissolution rate and oral bioavailability, Colloids Surf. B Biointerfaces 108 (2013) 366–373.
[17] M.A. Costa, R.C. Seiceira, C.R. Rodrigues, Efavirenz dissolution enhancement I: Co-micronization, Pharmaceutics 2013 (5) (2013) 1–22.
[18] B.V. Eerdenbrugh, B. Stuyven, L. Froyen, et al., Downscaling drug nanosuspension production: processing aspects and physicochemical characterization, AAPS PharmSciTech 10 (2009) 44–53.
[19] M. Bindu, B. Kusum, K. Chatanya, et al., Dissolution enhancement of efavirenz by solid dispersion and PEGylation techniques, Int. J. Pharm. Investig. 1 (2011) 29–34.
[20] A.M. Fatouh, A.H. Elshafeey, A. Abdelbary, Agomelatine-based insitu gels for brain targeting via the nasal route: statistical optimization, invitro, and invivo evaluation, Drug Deliv. 24 (1) (2017) 1077–1085.
[21] P.R. Ravi, N. Aditya, S. Patil, L. Cherian, Nasal in-situ gels for delivery of rasagiline mesylate: improvement in bioavailability and brain localization, Drug Deliv. 22 (7) (2015) 903–910.
[22] M.S. Mahajan, P.P. Nerkar, A. Agrawal, Nanoemulsion-based intranasal drug delivery system of saquinavir mesylate for brain targeting, Drug Deliv. 21 (2014) 148–154.
[23] N.A.H.A. Youssef, A.A. Kassem, R.M. Farid, F.A. Ismail, M.A.E. El-Massik, N.A. Boraie, A novel nasal almotriptan loaded solid lipid nanoparticles in mucoadhesive in situ gel formulation for brain targeting: preparation, characterization and in vivo evaluation, Int. J. Pharm. 548 (1) (2018 Sep 5) 609–624.
[24] E. Franciska, A.B. Luca, F. Daniel, B. Ägnes, G. Sveinbjorrn, Evaluation of intranasal delivery route of drug administration for brain targeting, Brain Res. Bull. 143 (2018) 155–170.
[25] D. Sharma, D. Maheshwari, G. Philip, et al., Formulation and optimization of polymeric nanoparticles for intranasal delivery of lorazepam using box-behnken design: in vitro and in vivo evaluation, BioMed Res. Int. 2014 (2014) 14. Article ID 156010.
[26] S.R. Pailla, S. Talluri, N. Rangaraj, et al., Intranasal Zotepine Nanosuspension: intended for improved brain distribution in rats, DARU J. Pharm. Sci. 27 (2019) 541–556.
[27] D.M. Brahmankar, S.B. Jaiswal, Biopharmaceutics and Pharmacokinetics-A Treatise, third ed., Vallabh Prakashan, 2015, pp. 256–257, 237-40.
[28] R.F. Bevill, L.W. Dittert, D.W.A. Bourne, Pharmacokinetics of sulfamethazine in cattle following IV and three oral dosage forms, J. Pharmacol. Sci. 66 (1977) 619–623.
[29] M. Franco, Efavirenz, Expet Opin. Pharmacother. 88 (2007) 1137–1145.
[30] S.P. Kakad, S.J. Kshirsagar, Development of reverse phase high-performance liquid chromatographic method for the estimation of HIV non-nucleoside reverse transcriptase inhibitor drug efavirenz in the rat brain, Futur. J. Pharm. Sci. 7 (2021) 11.
[31] A. Belgamwar, S. Khan, P. Yeole, Intranasal Chitosan HP-B-CD nanoparticles of efavirenz for the CNS targeting, Artif. Cells Nanomed. Biotechn. 46 (2) (2018) 374–386.
[32] Stability testing of active pharmaceutical ingredients and finished pharmaceutical products. Annex 10. WHO Expert Committee on Specifications for Pharmaceutical

Preparations Fifty-second report, Available online at: http://www.ich.org/fileadmin/Public_Web_Site/ICH_Products/Guidelines/Quality/Q1F/Q1F_Explanatory_Note.pdf.
[33] S. Honary, F. Zahir, Effect of zeta potential on the properties of nano-drug delivery systems - a review (Part 2), Trop. J. Pharmac. Res. 12 (2) (2013) 265–273.
[34] B.K. Ahuja, S.K. Jena, S.K. Paidi, et al., Formulation, optimization and in vitro–in vivo evaluation of febuxostat nanosuspension, Int. J. Pharm. 478 (Issue 2) (2015) 540–552. ISSN 0378-5173.
[35] S. Gänger, K. Schindowski, Tailoring formulations for intranasal nose-to-brain delivery: a review on architecture, physico-chemical characteristics and mucociliary clearance of the nasal olfactory mucosa, Pharmaceutics 1 (2018) 116.
[36] J.R. Authelin, M. Nakach, T. Tadros, et al., Engineering of nano-crystalline drug suspensions: employing a physico-chemistry based stabilizer selection methodology or approach, Int. J. Pharm. 476 (2) (2014) 277–288, 1.
[37] S. Talegaonkar, P.R. Mishra, Intranasal delivery: an approach to bypass the blood brain barrier, Int. J. Pharm. 36 (2004) 140–147.
[38] J. Weiss, J. Rose, C.H. Storch, et al., Modulation of human BCRP (ABCG2) activity by anti-HIV drugs, J. Antimicrob. Chemother. 59 (2007) 238–245.
[39] N. Apostolova, H.A. Funes, A.B. Garcia, et al., Efavirenz and the CNS: what we already know and questions that need to be answered, J. Antimicrob. Chemother. 70 (10) (2015) 2693–2708.